European Commission

JRC TECHNICAL REPORTS

Observables of interest for the characterisation of Spent Nuclear Fuel

Gašper Žerovnik
Peter Schillebeeckx
Kevin Govers
Alessandro Borella
Dušan Ćalić
Luca Fiorito
Bor Kos
Alexey Stankovskiy
Gert Van den Eynde
Marc Verwerft

2018

Joint Research Centre

EUR 29301 EN

This publication is a Technical report by the Joint Research Centre (JRC), the European Commission's science and knowledge service. It aims to provide evidence-based scientific support to the European policymaking process. The scientific output expressed does not imply a policy position of the European Commission. Neither the European Commission nor any person acting on behalf of the Commission is responsible for the use that might be made of this publication.

Contact information
Name: Peter Schillebeeckx
Address: Joint Research Center, Retieseweg 111, 2440 Geel, Belgium
Email: Peter.Schillebeeckx@ec.europa.eu
Tel.: +32 (0)14 571 475

JRC Science Hub
https://ec.europa.eu/jrc

JRC112361

EUR 29301 EN

PDF ISBN 978-92-79-90347-2 ISSN 1831-9424 doi:10.2760/418524

Luxembourg: Publications Office of the European Union, 2018

How to cite this report: G. Žerovnik et al., *Observables of interest for the characterization of Spent Nuclear Fuel*, EUR 29301 EN, Publications Office of the European Union, Luxembourg, 2018, ISBN 978-92-79-90347-2, doi 10.2760/418524, PUBSY No JRC112361.

Observables of interest for the characterisation of Spent Nuclear Fuel

G. Žerovnik[a], P. Schillebeeckx[a], K. Govers[b], A. Borella[b], D. Ćalić[c], L. Fiorito[b], B. Kos[c], A. Stankovskiy[b], G. Van den Eynde[b] and M. Vervwerft[b]

[a]European Commission (EC), Joint Research Centre (JRC),
Retieseweg 111, B-2440 Geel, Belgium

[b]SCK•CEN, Belgian Nuclear Research Centre,
Boeretang 200, B-2400 Mol, Belgium

[c]Jožef Stefan Institute (JSI),
Jamova cesta 39, SI-1000 Ljubljana, Slovenia

Contents

Abstract

The characterisation of Spent Nuclear Fuel (SNF) in view of intermediate storage and final disposal is discussed. The main observables of interest that need to be determined are the decay heat, neutron and γ-ray emission spectra. In addition, the inventory of specific nuclides that are important for criticality safety analysis and for verification of the fuel history has to be determined. Some of the observables such as the decay heat and neutron and γ-ray emission rate can be determined by Non-Destructive Analysis (NDA) methods. Unfortunately, this is not always possible especially during routine operation. Hence, a characterisation of SNF will rely on theoretical calculations combined with results of NDA methods. In this work the observables of interest, also referred to as source terms, are discussed based on theoretical calculations starting from fresh UO_2 and MOX fuel. The irradiation conditions are representative for PWR. The Serpent code is used to define the nuclides which have an important contribution to the observables. The emphasis is on cooling times between 1 a and 1000 a.

1 Introduction

While fresh fuel of a Light Water Reactor (LWR) consists mainly of oxides of a few uranium isotopes and in case of MOX also of plutonium isotopes, Spent Nuclear Fuel (SNF) contains a large number of nuclides. They are formed as a result of neutron induced reactions and radioactive decay occurring during neutron irradiation and cooling periods. Due to the presence of radionuclides a SNF assembly needs to be characterised for its decay heat and neutron and γ-ray emission for a safe, secure, ecological and economical transport, intermediate storage and final disposal. To avoid too conservative loading schemes, the inventory of strong neutron absorbing nuclides, including Fission Products (FP) and actinides, is also required. The concept of accounting for the presence of these nuclides in a (sub)-criticality analysis is referred to as BurnUp Credit (BUC). In addition, the amount of some specific nuclides such as ^{148}Nd and ^{149}Sm are important to verify the irradiation history of the assembly.

Some of the observables, i.e. decay heat and neutron and γ-ray emission rate, can be determined by Non-Destructive Analysis (NDA) methods. Unfortunately, a measurement of the decay heat of an assembly lasts at least one full day. This is too long for routine operations. In addition, to determine the inventory of specific nuclides for criticality safety assessments and for verification of the fuel history, theoretical calculations are required. Therefore, a full characterisation of a SNF assembly will rely on theoretical calculations combined with results of NDA measurements. The calculations involve a neutron transport code combined with a nuclide creation and fuel depletion code. The results of such calculations strongly depend on nuclear data, fuel fabrication data and reaction operation and irradiation conditions. In this report the components which have an impact on the observables of interest are identified and a list of key nuclides to determine them is defined. The emphasis is on cooling times between 1 year and a few hundreds of years.

2 Computational methods and reference models

To estimate the nuclide inventory of SNF a coupling of a neutron transport and nuclide production and depletion code is required. Neutron transport calculations have to be done at each time step during neutron irradiation to determine the spatial and energy distribution of the neutron fluence rate. These distributions are used to determine energy averaged neutron induced reaction cross sections, which are required for the nuclide production and fuel depletion step.

Neutron transport calculations can be performed in a deterministic way by solving the Boltzmann transport equation or in a stochastic way by performing Monte Carlo (MC) simulations. The depletion calculations are about solving the Bateman equations. The simplest approach to solve the equations is the matrix exponential method. It is based on a power series expansion of the equation system matrix and used by e.g. the ORIGEN module of the SCALE code system [1]. Modern depletion codes such as ALEPH2 [2] and Serpent [3] use more advanced methods, which significantly accelerate the convergence of the solution of the Bateman equations and allow a decreased number of time steps during the fuel irradiation with neutrons. After the end of the irradiation, i.e. during the cooling time period, the nuclide vector at any cooling time can be determined by accounting for the decay. This involves decay data which are recommended with rather low uncertainties [4][5][6].

The Serpent code [3] was used to calculate the nuclide inventory of a SNF sample originating from fresh UO_2 and MOX fuel. It uses an advanced depletion algorithm based on the predictor-corrector method coupled with a continuous energy MC neutron transport module. Since the Serpent code does not provide information on neutron emission from (α,n) reactions, the neutron production by (α,n) reactions was estimated using the SOURCES code [7]. This code was implemented in the ORIGEN-2.2 module of the SCALE code system [1]. The nuclear data required for the calculations, i.e. neutron induced interaction cross sections, neutron fission data (i.e. fission neutron multiplicities and FP yields) and radioactive decay data, were taken from the ENDF/B-VII.1 library [8].

The calculations were performed starting from fresh UO_2 and MOX fuel for the same geometry and irradiation conditions. The fuel is continuously irradiated for 1000 d at a constant linear pin power density of 250 W/cm. The geometry, a two-dimensional 3×3 fuel pin configuration with reflective boundary conditions, is illustrated in Figure 1. A single fuel pin consists of 4 concentric regions and an outer coolant/moderator region:

1. The fuel in the inner region is at a temperature of 900 K, with a 5 g/cm linear density and 0.4057 cm radius. The composition of the fresh UO_2 and MOX fuel is specified in Table 1.
2. The fuel is surrounded by a 0.043 mm thick ^{4}He layer at a temperature of 900 K with a density of 0.0013 g/cm^3.
3. Outside of the helium layer is a cladding layer at a temperature of 600 K, with a density of 6.53 g/cm^3 and an inner and outer radii of 0.41 cm and 0.465738 cm, respectively. The cladding is an alloy containing 98.3 wt% Zr.
4. The cladding is surrounded by a 0.02556 mm thick Ni-alloy layer representing the height-averaged fuel assembly grid, at a temperature of 600 K and with a density of 8.08 g/cm^3.
5. The outermost region consists of water at a temperature of 573.8 K, with a density of 0.675 g/cm^3 containing 400 ppm boron. The spacing between the neighbouring pins is 1.243796 cm.
6. The 3×3 pin array is surrounded by a zirconium alloy and water layer with a thickness of 0.01 cm and 0.07216 cm, respectively.

These conditions are representative for an irradiation in a Pressurised Water Reactor (PWR). All fuel pins are depleted, but only the composition of the central pin is observed.

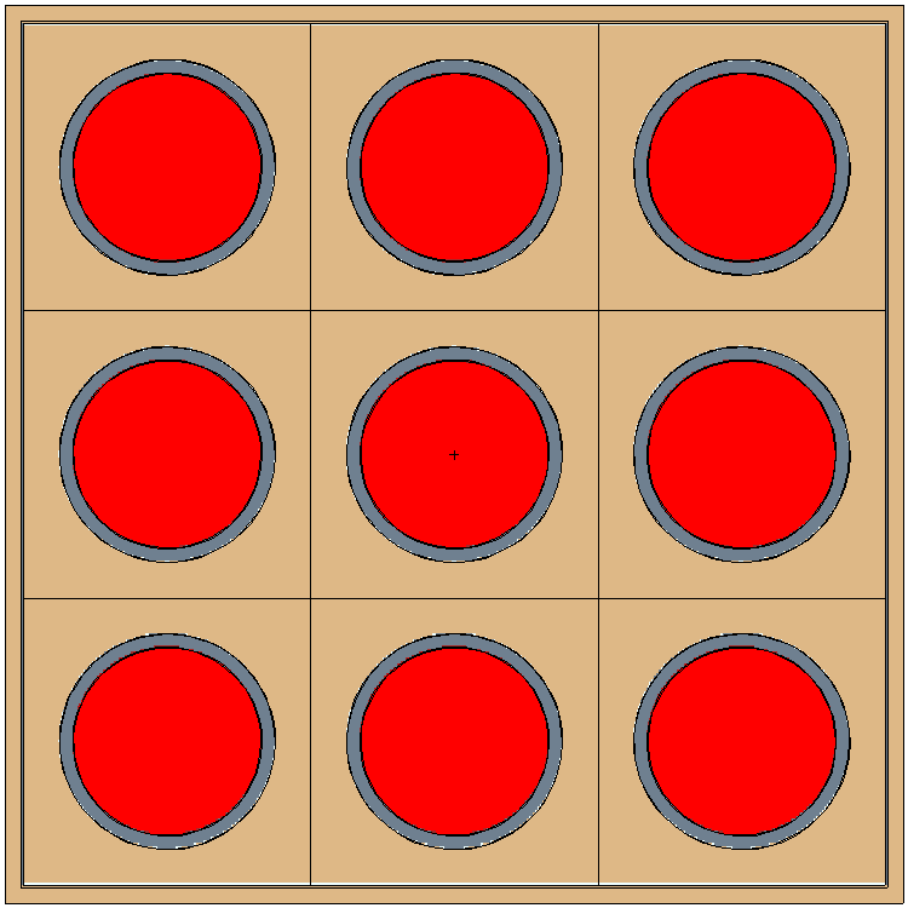

Figure 1: The two dimensional 3×3 fuel pin geometry used for the calculations presented in this work. The geometry is explained in the text.

Table 1: The weight fraction of U and Pu isotopes in the fresh UO_2 and MOX fuel used for the calculations in this report. The weight fractions are normalised to the total amount of U and Pu. The isotopic composition of oxygen in the calculations is based on the recommended natural abundances.

Nuclide	Weight fraction	
	UO_2	MOX
^{234}U	0.00045	0.0000092
^{235}U	0.04794	0.0023
^{236}U	0.00001	0
^{238}U	0.95159	0.9176908
^{238}Pu	0	0.002
^{239}Pu	0	0.04376
^{240}Pu	0	0.02088
^{241}Pu	0	0.0076
^{242}Pu	0	0.00576

Computer codes can introduce bias effects due to numerical approximations related to both the neutron transport and nuclide creation and fuel depletion codes. Neutron transport codes based on MC simulations, in contrast to deterministic codes, do not require a discretisation of the energy, direction and spatial variables, and are therefore more accurate. However, discretisation of the time step cannot be avoided when calculating the fuel depletion. The following approximations have been adopted:

- At each time step during neutron irradiation, two MC simulations, corresponding to the predictor and the corrector step, with 5000 neutrons in 500 active neutron cycles each are performed, i.e. 5×10^6 simulated neutron histories per time step. The resulting relative MC counting statistics uncertainties for the ^{244}Cm concentration and decay heat are less than 0.7% and 0.03%, respectively.
- The initial fission neutron source was uniformly distributed over all fuel regions and 10 neutron cycles were used to converge the fission neutron source.
- The neutron irradiation time steps, in chronological order, are: 4 × 25 d, 4 × 50 d and 7 × 100 d. This results in a relative uncertainty of the ^{244}Cm concentration of 0.5% and <0.1% for the total decay heat rate.
- To account for neutron self-shielding effects the central fuel pin was divided into 4 regions. For the fuel depletion of the surrounding pins no self-shielding was taken into account.

3 Observables

The observables of interest for transport, intermediate storage and final disposal of SNF, i.e. decay heat, neutron and γ-ray emission and the nuclide inventory to account for BUC and to verify the fuel history, are studied. The study is based on calculations for the fresh UO_2 and MOX fuel and irradiation conditions described in Section 2. Information about the nuclide inventory at the end of the irradiation and at different cooling times is given in Appendix A.

3.1 Decay heat rate

The decay heat of SNF originates from the decay of the radionuclides present in the fuel. SNF consists of thousands of different radionuclides with a broad range of half-lives – from fractions of a second to billions of years. During operation of a LWR the decay heat contributes for about 4% to the total thermal power that is produced [9]. Due to this decay heat, active cooling is required for weeks after reactor shutdown to prevent SNF melting. Therefore, decay heat is an important factor affecting nuclear safety.

The decay heat of SNF is also of primary importance to optimise the interim storage and final disposal of SNF. This involves studies of the decay heat for cooling times between 1 a and 1000 a. The decay heat rate density p_r emitted by SNF can be calculated by:

$$p_r = \sum_i E_{ri}\,\lambda_i\,n_i \quad , \tag{1}$$

where E_{ri} is the recoverable heat per decay, λ_i is the decay constant and n_i is the number density of the nuclide i. Hence, three components contribute to the uncertainty of the decay heat rate.

The decay constants λ_i for nuclides with half-lives >1 a are mostly well known and their contribution to the decay heat rate uncertainty can practically be neglected. The decay of a radionuclide by the emission of a charged particle, such as an α- or β-particle, usually leaves the daughter nucleus in an excited state. In most cases, this results in the emission of γ-rays. One usually assumes that the energy of the γ-rays involved in the decay processes can be fully transferred into heat. Hence, in case of α-decay the energy E_{ri} is the total disintegration energy or Q-value, which is known with relatively low uncertainties. However, in case of β-decay a fraction of the disintegration energy is transferred into (anti)neutrino energy. This energy will not be converted into heat and the energy dissipated into heat is determined by the energy distribution of the emitted γ-rays and electrons. No recommended values together with uncertainties can be found in the literature for the recoverable heat for nuclides of interest decaying by β-decay. In addition, the kinetic energy of emitted electrons or γ-rays is not always transferred into measured heat. Some of this energy might be lost due to γ-rays that escape from the measurement system or due to electrons producing Bremsstrahlung escaping partly from the system. The fraction that is lost depends on the γ-ray or Bremsstrahlung energy and the material composition of the environment. To estimate the uncertainty due to the number density n_i a detailed sensitivity analysis combined with an uncertainty propagation scheme is required.

The SNF decay heat rate as a function of cooling time for a SNF resulting from the irradiation of a fresh UO_2 and MOX fuel under the conditions described in Section 2 is presented in Figure 2. The decay heat due to individual contribution of α- and β-particles and γ-rays is shown Figure 3. The relative contributions of individual radionuclides are emphasised in Figure 4. Detailed information on the main contributions to the decay heat at different cooling times is given in Appendix B.

The total decay heat rate for SNF originating from fresh MOX fuel is larger compared to the one from SNF originating from UO_2 fuel. This is due to the contribution of the actinides (Pu, Am, Cm) when starting with MOX fuel. The largest contribution for cooling times between 1 a and 10 a is due to relatively short-lived FP chains, mainly ^{144}Ce/^{144}Pr

and $^{106}Ru/^{106}Rh$. The contribution of actinides is only significant in case of MOX fuel. For MOX fuel the contributions from ^{242}Cm and ^{244}Cm exceed 10%. For cooling times between 10 a and 30 a, the contributions from the short-lived FP chains become negligible. For UO_2 fuel, the decays of $^{90}Sr/^{90}Y$ and $^{137}Cs/^{137m}Ba$ have the largest contribution to the total decay heat. In case of MOX, the largest contribution is due to the decay of ^{244}Cm, followed by ^{238}Pu and ^{241}Am. With increasing cooling time the contribution from ^{241}Am becomes the dominant one. This is due to build-up of ^{241}Am by ^{241}Pu decay. Even though the relative contribution of the $^{137}Cs/^{137m}Ba$ decay is much smaller for MOX fuel, its absolute value is comparable to the one for UO_2 fuel. On the other hand, the contribution of the $^{90}Sr/^{90}Y$ decay is also smaller in absolute terms due to the lower cumulative yield of ^{90}Sr for neutron induced fission of ^{239}Pu and ^{241}Pu compared to the FP yields for neutron induced fission of ^{235}U. For cooling times longer than 50 a, the decay heat for both SNF types is dominated by the contribution from the decay of ^{241}Am. Other contributions are due to the decay of $^{238,239,240}Pu$. The contributions from light nuclides are getting smaller and eventually become negligible for cooling times longer than about 300 a.

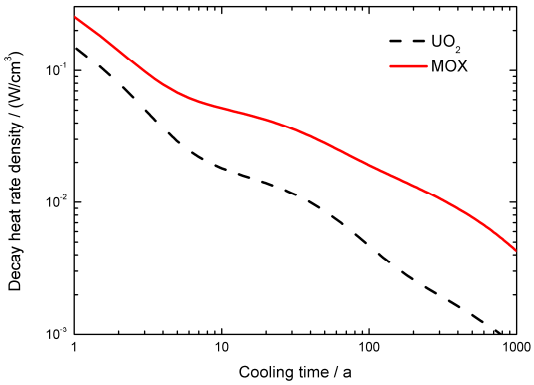

Figure 2: Decay heat rate density as a function of cooling time for a SNF sample resulting from the irradiation of UO_2 and MOX fresh fuel under the conditions described in Section 2.

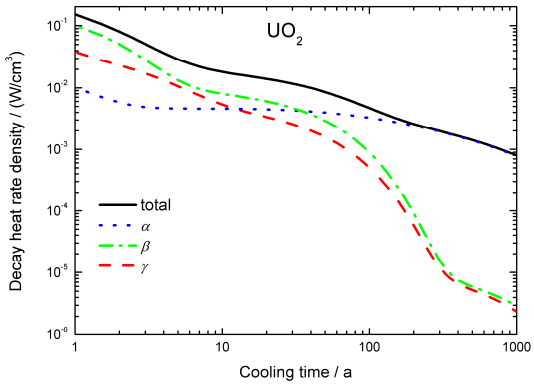

Figure 3: Decay heat rate density as a function of cooling time for a SNF sample resulting from the irradiation of fresh UO_2 fuel. Contributions due to the emission of γ-rays and α- and β-particles are also plotted.

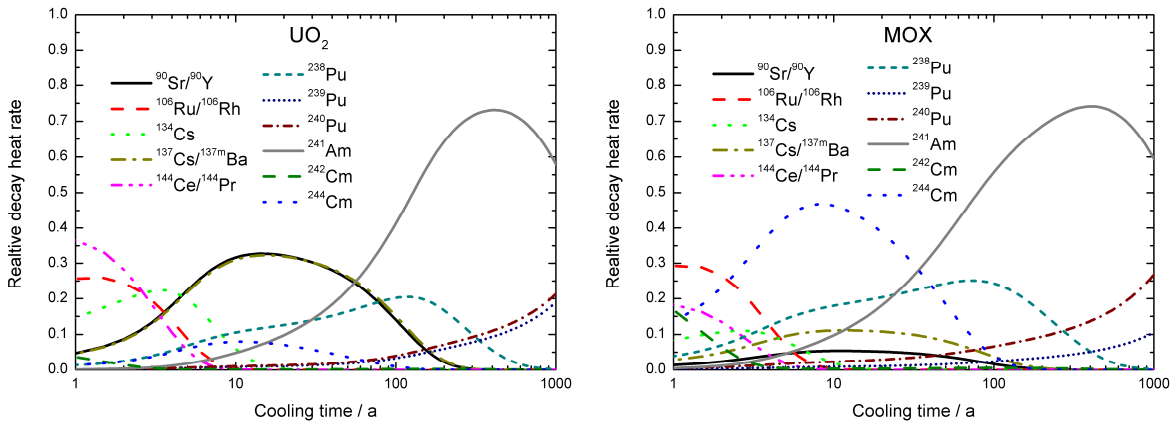

Figure 4: Relative contribution of radionuclides to the total decay heat as a function of cooling time. The SNF originates from the irradiation of fresh UO_2 (left) and MOX (right) fuel under the conditions described in Section 2.

3.2 Photon emission rate, energy density and spectra

The γ-ray emission rate spectrum per unit volume, denoted by $s_\gamma(E)$, can be obtained from the nuclide inventory by:

$$s_\gamma(E) = \sum_{i,j} P_{\gamma ij}\,\delta(E - E_{\gamma ij})\,\lambda_i n_i \ , \tag{2}$$

where $P_{\gamma ij}$ is the emission probability of a photon with energy $E_{\gamma ij}$ per decay of the nuclide i and $\delta(x)$ is the Dirac delta distribution. The photon emission rate energy density $\varphi_{q\gamma}(E)$ is defined as:

$$\varphi_{q\gamma}(E) = s_\gamma(E)E \ . \tag{3}$$

The total γ-ray emission rate energy density becomes:

$$\Phi_{q\gamma}(E) = \int_0^\infty s_\gamma(E)E\,dE_\gamma \ . \tag{4}$$

Most of the decay constants and γ-ray emission probabilities and energies of interest are recommended with relatively small uncertainties. The main contribution to the uncertainty of the calculated photon emission rate energy density (Eq. 4) is due to uncertainty of the number density n_i.

Figure 5 shows the energy dependence of the γ-ray emission rate energy density $\varphi_{q\gamma}(E)$ for SNF originating from fresh UO_2 fuel. Only the contribution of γ-rays with an energy E > 400 keV is presented. The total γ-ray emission rate energy density is plotted as a function of cooling time in Figure 6.

For cooling times < 10 a, the γ-ray spectrum is dominated by γ-rays originating from the decay of relatively short-lived FP, i.e. the decay of ^{95}Zr, ^{95}Nb, ^{106}Ru/^{106}Rh and ^{144}Ce/^{144}Pr. There is also a contribution of 511 keV γ-rays due to electron-positron annihilation following β^+ decays. For cooling times between 10 a and 30 a, the most prominent γ-rays originate from the decay of ^{134}Cs, ^{137}Cs/^{137m}Ba and ^{154}Eu [10]. For larger cooling times, i.e. between 30 a and 200 a, the 661 keV γ-ray due to the ^{137}Cs/^{137m}Ba decay dominates the spectrum. For cooling times > 400 a there is practically only a contribution of γ-rays with an energy < 400 keV due to the decay of ^{241}Am, as illustrated in Figure 6. They will be absorbed by the fuel and will not contribute to the dose rate.

The discussion of the spectra in Figure 5 and Figure 6 reveal that the γ-ray spectra for cooling times < 100 a are dominated by the decay of FP. Therefore, γ-ray spectra emitted by SNF originating from fresh MOX fuel are very similar. Some differences occur due to differences in FP yields for neutron induced fission of ^{235}U and ^{239,241}Pu.

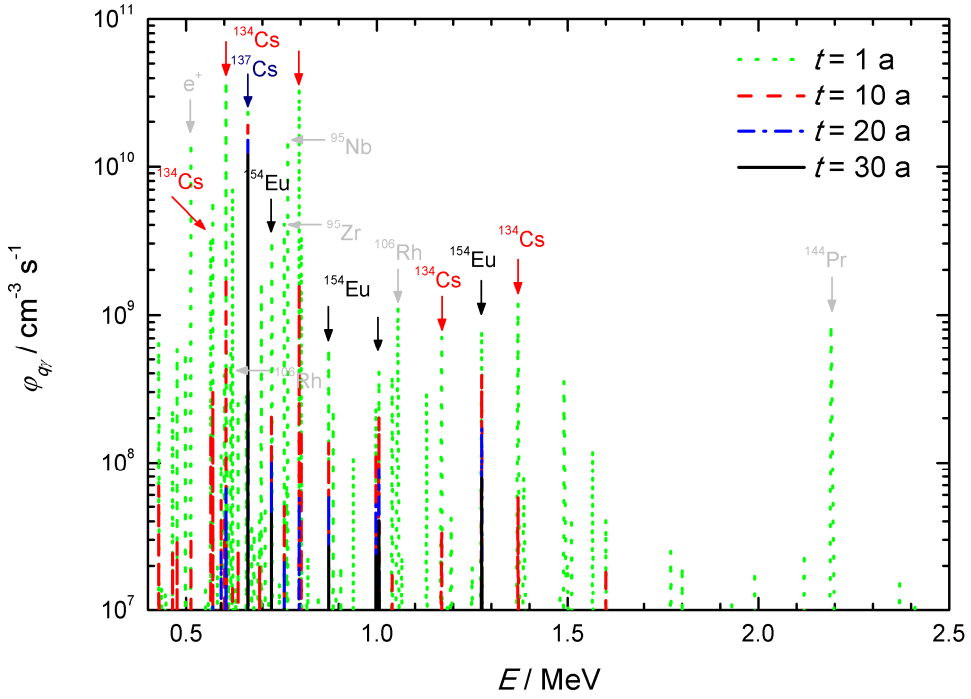

Figure 5: Energy dependence of the γ-ray emission rate energy density $\varphi_{q\gamma}(E)$ by a SNF sample originating from the irradiation of fresh UO_2 fuel under the conditions specified in Section 2.

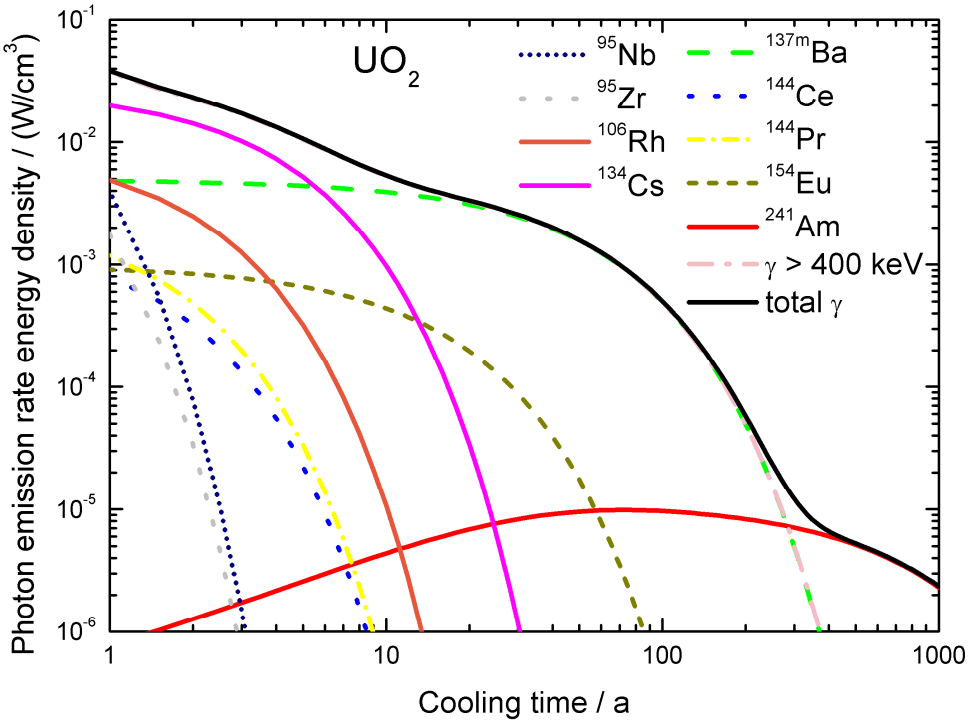

Figure 6: Total γ-ray emission rate energy density together with the contributions of some radionuclides as a function of cooling time of SNF originating from the irradiation of fresh UO_2 fuel under the conditions specified in Section 2.

3.3 Neutron emission rate

The total neutron emission rate density s_n from SNF is the sum of contributions due to spontaneous fission (SF) and (α,n) reactions:

$$s_n = \sum_i (s_{SF,i} + s_{\alpha,i})\, n_i \ . \tag{5}$$

The specific neutron emission rate per nucleus due to SF and (α,n) reactions following the decay of nuclide i are denoted by $s_{SF,i}$ and $s_{\alpha,i}$, respectively. The specific SF neutron emission rate is given by:

$$s_{SF,i} = \langle \nu \rangle_i \lambda_{SF,i} \ , \tag{6}$$

where $\langle \nu \rangle_i$ is the total number of neutrons emitted per SF and $\lambda_{SF,i}$ is the decay constant for SF of the nuclide i. The production of neutrons by (α,n) reactions is mostly treated under the assumption of an infinitely thick target, i.e. the thickness is sufficient to completely stop α-particles. The specific neutron emission rate due to α-decay of nuclide i becomes:

$$s_{\alpha,i} = \lambda_{\alpha,i} \sum_l \sum_k P(E_{\alpha k}) Y_l(E_{\alpha k}) \ , \tag{7}$$

where $\lambda_{\alpha,i}$ is the decay constant for α-decay of nuclide i, $P(E_{\alpha k})$ the probability that an α-particle is emitted with an energy $E_{\alpha k}$ by nuclide i and $Y_l(E_{\alpha k})$ is the neutron yield for an α-particle with an energy $E_{\alpha k}$. The latter is the number of neutrons produced per incident α-particle interacting with a material with number density n_l. The neutron yield Y_l can be expressed as:

$$Y_l(E_\alpha) = N_l \int_0^{E_\alpha} \frac{\sigma_l(\alpha,n)}{\frac{dE}{dx}} dE_\alpha \ , \tag{8}$$

where $\sigma_l(\alpha, n)$ is the neutron production cross section for target nucleus l and dE/dx is the linear stopping power of the target material.

Neutron emission by SNF is predominantly due to spontaneous fission of heavy nuclides, in particular ^{242}Cm and ^{244}Cm, and (α,n) reactions due to mainly the presence of oxygen. For most of the actinides, the SF decay constants and total neutron emission probabilities are recommended with uncertainties of less than 1.5% and 0.5%, respectively. The main uncertainty component for neutron emission due to SF is the uncertainty of the number densities of the actinides. Thick target yields for (α,n) reactions in nuclear material have recently been reviewed by Simakov and van den Berg [11]. The recommended thick target yields are given with an uncertainty of 8.1% and 8.6% for UO_2 and PuO_2 target materials, respectively. These uncertainties are definitely not negligible compared to the uncertainty of the number density of the contributing nuclides.

The total neutron emission rate together with the contributions due to SF and (α,n) reactions are shown in Figure 7 as a function of cooling time. The neutron emission rate for SNF originating from fresh MOX fuel is about one order of magnitude larger compared to the one originating from fresh UO_2 fuel. For SNF originating from MOX, the SF neutrons are the dominating neutron source. For SNF originating from UO_2 fuel, neutrons from SF dominate the neutron production for cooling times <100 a. For cooling times between 100 a and 500 a there is a relatively strong contribution from (α,n) reactions.

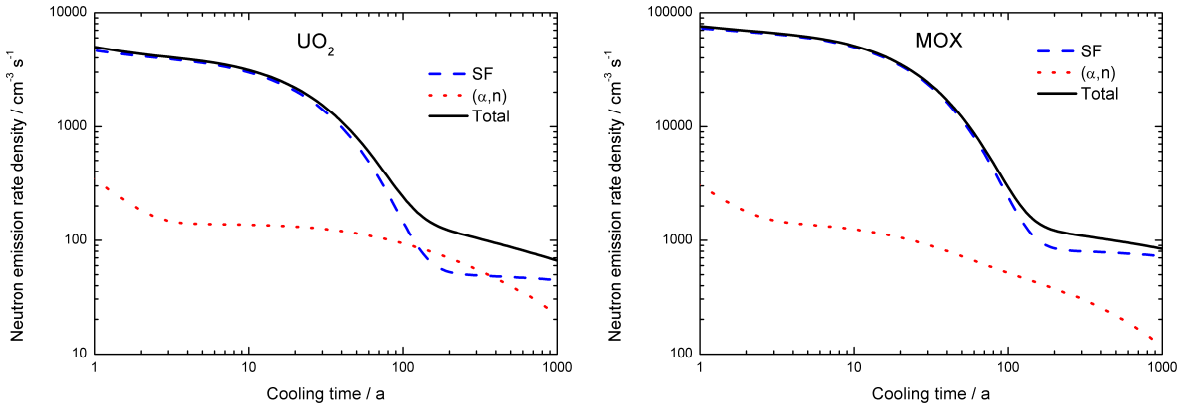

Figure 7: Neutron emission rate density, together with the contribution due to SF and (α,n) reactions, as a function of cooling time for SNF originating from fresh UO_2 (left) and MOX (right) fuel.

Figure 8 shows the relative contributions of specific nuclides to the neutron emission originating from spontaneous fission as a function of cooling time. Due to its relatively short half-life, i.e. $T_{1/2}$ = 0.446 a, ^{242}Cm is only important for short cooling times. The dominant contributor to the SF neutron emission rate for cooling times up to about 100 a is ^{244}Cm. For cooling times between 100 a and 1000 a, the most important contributor is ^{246}Cm, followed by ^{240}Pu and ^{242}Pu. For SNF originating from MOX fuel, the contribution of ^{246}Cm relative to ^{240,242}Pu is higher compared to SNF from UO_2 fuel, due to the much higher build-up of ^{246}Cm.

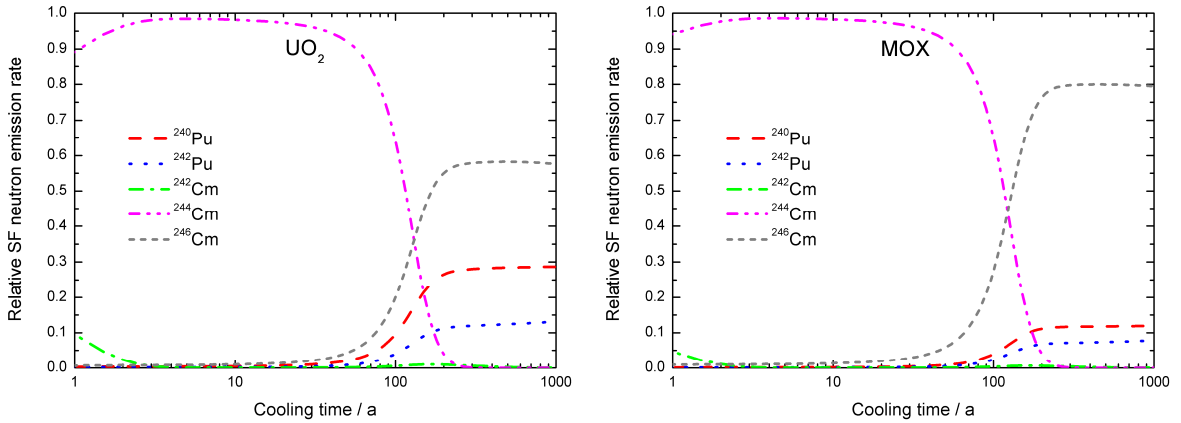

Figure 8: Relative contribution of ^{240,242}Pu and ^{242,244,246}Cm to the total SF neutron emission rate as a function of cooling time. The results are shown for SNF originating from UO_2 (left) and MOX (right) fuel.

The contributions to the neutron emission rate by (α,n) reactions are mainly due to the α-decay of ^{238,239,240}Pu, ^{241}Am and ^{242,244}Cm. Their relative contributions to the neutron emission by (α,n) reactions are plotted as a function of cooling time in Figure 9. The contribution of ^{242}Cm to the neutron emission by (α,n) reactions is only important for short cooling times when the total (α,n) contribution to the total emission rate is very small. For cooling times between 2 a and 30 a, the most important contribution to the (α,n) neutrons comes from the α-decay of ^{238}Pu and ^{240}Pu followed by the decay of ^{241}Am. For even longer cooling times the relative contribution of ^{241}Am increases. For cooling times > 300 a, contributions from ^{239,240}Pu become relatively more important.

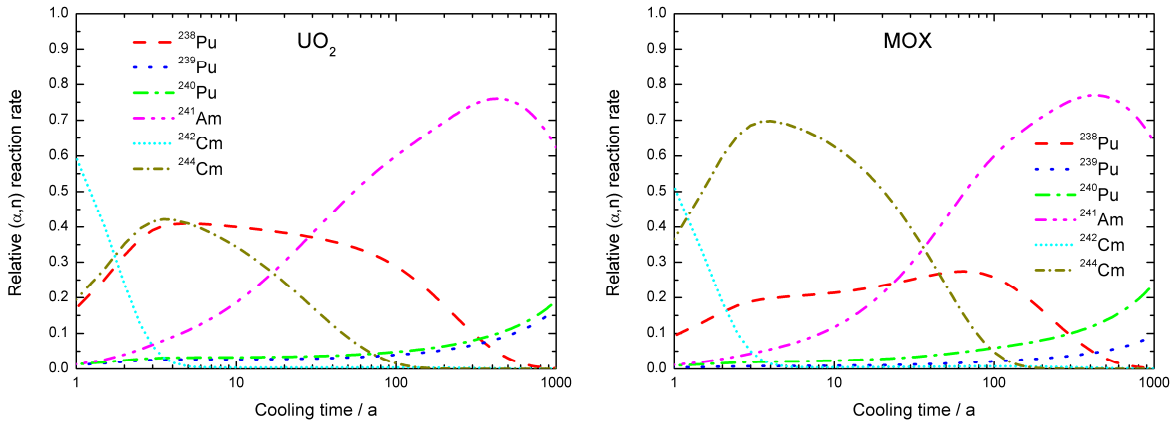

Figure 9: Relative contribution of ^{238,239,240}Pu, ^{241}Am and ^{242,244}Cm to the total neutron emission by (α,n) reactions as a function of cooling time. The results are shown for SNF originating from UO_2 (left) and MOX (right) fuel.

3.4 Burnup and power indicators

BurnUp (BU) of SNF is used as a measure for the total energy that is produced by nuclear fuel during reactor operation. Evidently it is directly related to the total number of neutron induced fission reactions that occurred. An ideal BU indicator is a parameter that is directly proportional to the thermal power and is not sensitive to other irradiation conditions or fuel history parameters such as fuel composition, power density and cooling time. The total number of ^{148}Nd nuclei produced during irradiation is often used as a BU indicator. It is produced by neutron induced fission or by decay of very short lived fission products ($T_{1/2}$ < 2 min) such that its production rate is proportional to the total fission rate. In addition, it is stable and has a relatively low cross section for neutron absorption. Hence, its removal during irradiation is negligible and its concentration is independent of cooling time. For a given incident neutron energy the relative difference in cumulative fission yields for neutron induced fission of ^{235}U and ^{239}Pu is within 0.3% [4]. The cumulative fission yields of ^{148}Nd for neutron induced fission of ^{238}U, ^{241}Pu and ^{241}Am are significantly higher. Therefore, the ^{148}Nd concentration depends on the type of fuel, i.e. UO_2 or MOX, and type of reactor, i.e. fuel-to-moderator ratio that affects the neutron energy distribution. However, it is not sensitive to changes of fuel composition during neutron irradiation or to small variations in the fresh fuel composition. Other nuclides that are commonly used as BU indicators are the ratio of the number of ^{137}Cs and ^{134}Cs nuclei [12] and the total number of ^{139}La [13] and ^{244}Cm [12] nuclei that are produced.

Unlike BU, thermal reactor power can be accurately measured. However, local power variations can be measured only indirectly. Some reactor designs enable insertion of dosimeters at different positions in the core during reactor operation to assess the spatial power distribution. Alternatively, the local thermal reactor power density can be estimated from concentrations of so-called power indicators in SNF. The concentration of an ideal power indicator reaches equilibrium very quickly, i.e. within hours or days. Under these conditions, its equilibrium concentration is a function of power density and is not sensitive to other operation parameters, such as fuel composition and burnup. A relatively good candidate for a power indicator is ^{149}Sm. It is predominantly produced by decay of the short-lived ^{149}Pm ($T_{1/2}$ = 2.21 d), which is produced by a sequence of decays of very short-lived FP, i.e. ^{149}Pr and ^{149}Nd. The production rate of ^{149}Pm is proportional to the total fission rate and the ^{149}Pr FP yield. Due to its high thermal absorption cross section (4000 b), the ^{149}Sm concentration reaches equilibrium after about 1 week of operation of a typical power reactor at full power [9]. The equilibrium concentration is a function of the fission rate, which is assumed to be proportional to the reactor power. Since ^{149}Sm is a stable nuclide, its concentration is independent of the

cooling time after all the ^{149}Pm nuclei have decayed. However, due to significant differences in cumulative fission yields for neutron induced fission of different actinides, the ^{149}Sm concentration depends on the type of fuel. Additionally, due to the strong energy dependence of the ^{149}Sm absorption cross section, the ^{149}Sm concentration depends also on the neutron spectrum. Hence, significant differences in ^{149}Sm concentrations in SNF originating from UO_2 and MOX fuel are expected. Another candidate for a power indicator is ^{135}Xe. It has an even higher absorption cross section and a quicker response time than ^{149}Sm. It reaches equilibrium within 1 day. However, it can only be detected within the first few days after the end of neutron irradiation due to its short half-live ($T_{1/2}$ = 9.1 h).

3.5 Reactivity

A safe transport, storage and disposal of SNF requires a (sub)-criticality safety analysis. To avoid unnecessarily over-engineered and expensive transport and storage casks, the loading scheme needs to account for the reduction in nuclear reactivity of the SNF. This reduction is due to the net reduction of fissile nuclides (fuel depletion) and the production of non-fissile, strong absorbing actinides and fission products. The concept of taking credit for the reduction in reactivity is referred to as burnup credit (BUC). Hence, criticality safety assessments for SNF management considering BUC require a nuclide inventory prediction and nuclear reactivity calculations involving far more nuclides than would be considered in a conservative approach based on the inventory of the fresh fuel. Nuclides which strongly affect the BUC of a SNF assembly, are: ^{235,236,238}U, ^{239,240,241}Pu, ^{95}Mo, ^{99}Tc, ^{101}Ru, ^{103}Rh, ^{109}Ag, ^{133}Cs, ^{147,149,150,151,152}Sm [14].

4 Nuclide vector of importance

From the discussion in Section 3 the nuclides that are important for the characterisation of SNF can be identified. The list of nuclides for which the inventory in SNF has to be calculated is summarised in Table 2. Nuclides that are only important for BUC are not included. The table includes the half-life, the observable of interest and the nuclear data of importance.

Table 2: List of nuclides important for the characterisation of SNF. Cooling times between 1 a and 1000 a were considered. The table includes the half-life ($T_{1/2}$), the observable of interest and the nuclear data of importance.

Nuclide(s)	$T_{1/2}$	Decay heat	n emiss.	γ-ray emiss.	BU	Power indic.	BUC	ND
^{90}Sr/^{90}Y	28.8 a	×						Y_f, E_r
^{106}Ru/^{106}Rh	1.017 a	×		×				
^{133}Cs	stable						×	Y_f, σ_γ
^{134}Cs	2.065 a	×		×				σ_γ
^{137}Cs/^{137m}Ba	30.07 a	×		×				Y, E_r
^{144}Ce/^{144}Pr	284.6 d	×		×				
^{148}Nd	stable				×			
^{149}Sm	stable					×	×	
^{154}Eu	8.60 a			×				
^{238}Pu	87.7 a	×	×					
^{239}Pu	2.410 × 10^4 a						×	σ_γ
^{240}Pu	6.56 × 10^3 a						×	σ_γ
^{241}Pu	14.29 a						×	σ_γ
^{241}Am	432.7 a	×	×					
^{244}Cm	18.1 a	×	×					σ_γ

5 Conclusion

The characterisation of SNF in view of a safe, secure, ecological and economical intermediate storage and final disposal of SNF was discussed. The main observables of interest that have to be determined are the decay heat and neutron and γ-ray emission rate. In addition, the inventory of fissile nuclides and fission products with large absorption cross sections are required for criticality safety assessments and the inventory of other specific fission products such as ^{148}Nd and ^{149}Sm can be used as burnup and power indicators.

The list is based on theoretical calculations using the Serpent code. This code couples a neutron transport MC simulation code to a nuclide production and depletion code. The calculations were performed starting from fresh UO_2 and MOX fuel, with a fuel design and irradiation conditions that are representative for a PWR.

The results of the calculations reveal that for a cooling time between 10 a and 100 a the most important contributors to

- the decay heat are: ^{90}Sr/^{90}Y, ^{137}Cs/^{137m}Ba, ^{238}Pu, ^{241}Am and ^{244}Cm;
- the γ-ray emission rate are: ^{134}Cs, ^{137m}Ba and ^{154}Eu; and
- the neutron emission rate are: ^{238}Pu, ^{241}Am and ^{244}Cm.

The results of this report, i.e. list of key nuclides, will be used for a further sensitivity analysis to define realistic confidence limits and to identify nuclear data that need to be improved.

References

[1] Oak Ridge National Laboratory (ORNL), "Scale: A Comprehensive Modeling and Simulation Suite for Nuclear Safety Analysis and Design, Version 6.1," Report ORNL/TM-2005/39, Available from Radiation Safety Information Computational Center at Oak Ridge National Laboratory as CCC-785 (2011).

[2] A. Stankovskiy, G. Van den Eynde and L. Fiorito, "ALEPH v2.6, A Monte Carlo Burn-up Code," User's Manual, Restricted Contract Report SCK•CEN-R-5598, revision 2.6.3 (2015).

[3] J. Leppänen, "Serpent – a Continuous-energy Monte Carlo Reactor Physics Burnup Calculation Code," User's Manual, VTT Technical Research Centre of Finland (2015).

[4] A.L. Nichols, "Nuclear Data Requirements for Decay Heat Calculations," Workshop on Nuclear Data and Nuclear Reactors: Physics, Design and Safety, Trieste, 25 February – 28 March 2002, pp. 67-195.

[5] N. Kocherov, M. Lammer and O. Schwerer, "Handbook of nuclear data for safeguards," Report INDC(NDS)-0376, IAEA (1997).

[6] A.L. Nichols, D.L. Aldama and M. Verpelli, "Handbook for nuclear data for safeguards: database extensions, August 2008," Report INDC(NDS)-0534, IAEA (2008).

[7] W.B. Wilson, R.T. Perry, W.S. Charlton and T.A. Parish, "Sources: A code for calculating (alpha, n), spontaneous fission, and delayed neutron sources and spectra," Prog. Nucl. Energ. 51 (2009) 618-613.

[8] M.B. Chadwick et al., "ENDF/B-VII.1 Nuclear Data for Science and Technology: Cross Sections, Covariances, Fission Product Yields and Decay Data," Nucl. Data Sheets 112, 2887-2996 (2011).

[9] J.J. Duderstadt and L.J. Hamilton, "Nuclear reactor analysis," John Wiley & Sons, Inc. (1976).

[10] C. Willmann, "Applications of Gamma Ray Spectroscopy of Spent Nuclear Fuel for Safeguards and Encapsulation," Ph.D. thesis, University of Uppsala (2006).

[11] S. Simakov and Q.Y. van den Berg, "Update of the *α-n* Yields for Reactor Fuel Materials for the Interest of Nuclear Safeguards," Nucl. Data Sheets 139 (2017) 190-203.

[12] A.S. Chesterman, A. Simpson and M. Clapham, "Burnup Credit Measurements for Cask Loading Compliance – A Review of Techniques and Calibration Philosophies," In: Proc. Int. Conf. WM2011, paper No. 11194, Phoenix, USA (2011).

[13] G. Ilas and I.C. Gauld, "Analysis of Experimental Data for High-Burnup PWR Spent Fuel Isotopic Validation— Vandellós II Reactor," Report NUREG/CR-7013 ORNL/TM-2009/321, Oak Ridge National Laboratory (2011).

[14] A.S. Chesterman, M.J. Clapham and N. Gardner, "Radiometric characterisation supports, burnup credit, safeguards and radionuclide inventory determination for spent fuel transport, storage and disposal," Report IAEA-SM-253/35. In: Book of Extended Synopses, International Symposium on. Storage of Spent Fuel from Power Reactors, Vienna, Austria (1998).

List of abbreviations and definitions

BU	BurnUp
BUC	BurnUp Credit
EC	European Commission
ENDF/B	Evaluated Nuclear Data File/B-version
FP	Fission Product
IAEA	International Atomic Energy Agency
JRC	Joint Research Centre
JSI	Jožef Stefan Institute
LWR	Light Water Reactor
MC	Monte Carlo
MOX	Mixed Oxide
NDA	Non-Destructive Analysis
ND	Nuclear Data
NEA	Nuclear Energy Agency
OECD	Organisation for Economic Co-operation and Development
PWR	Pressurized Water Reactor
SCALE	Standardized Computer Analyses for Licensing Evaluation
SCK•CEN	Belgian Nuclear Research Centre
SF	Spontaneous Fission
SNF	Spent Nuclear Fuel

List of figures

List of tables

Appendix A. Nuclide vector tables

Table A.1: Inventory of nuclides of importance for the characterisation of SNF at the end of the irradiation of fresh UO_2 and MOX fuel. The composition of the fresh fuel and irradiation conditions are described in Section 2.

Nuclide i (half-life)	Number density n_i / (10^{24} cm^{-3})	
	UO_2 fuel	MOX fuel
^{90}Sr (28.8 a)	5.293×10^{-5}	2.581×10^{-5}
^{133}Cs (stable)	7.045×10^{-5}	7.145×10^{-5}
^{134}Cs (2.065 a)	1.054×10^{-5}	1.009×10^{-5}
^{137}Cs (30.07 a)	7.751×10^{-5}	7.916×10^{-5}
^{148}Nd (stable)	2.198×10^{-5}	2.199×10^{-5}
^{149}Sm (stable)	1.040×10^{-7}	3.304×10^{-7}
^{154}Eu (8.60 a)	1.941×10^{-6}	3.518×10^{-6}
^{235}U (7.04×10^{8} a)	2.680×10^{-4}	2.591×10^{-5}
^{236}U (2.342×10^{7} a)	1.625×10^{-4}	6.932×10^{-6}
^{238}U (4.468×10^{9} a)	2.261×10^{-2}	2.159×10^{-2}
^{238}Pu (87.7 a)	8.601×10^{-6}	4.079×10^{-5}
^{239}Pu (2.410×10^{4} a)	1.999×10^{-4}	6.034×10^{-4}
^{240}Pu (6.56×10^{3} a)	6.507×10^{-5}	4.219×10^{-4}
^{241}Pu (14.29 a)	4.714×10^{-5}	2.515×10^{-4}
^{242}Pu (3.75×10^{5} a)	1.643×10^{-5}	1.590×10^{-4}
^{241}Am (432.7 a)	1.194×10^{-6}	1.448×10^{-5}
^{242g}Am (16.02 h)	4.148×10^{-9}	2.526×10^{-8}
^{242m}Am (141 a)	1.287×10^{-7}	1.332×10^{-6}
^{243}Am (7.37×10^{3} a)	3.831×10^{-6}	4.103×10^{-5}
^{242}Cm (0.446 a)	5.325×10^{-7}	4.051×10^{-6}
^{243}Cm (29.1 a)	1.852×10^{-8}	2.052×10^{-7}
^{244}Cm (18.1 a)	1.847×10^{-6}	3.069×10^{-5}

Table A.2: Inventory of nuclides of importance for the characterisation of SNF after irradiation of fresh UO_2 and MOX fuel and a cooling time of 1 a. The composition of the fresh fuel and irradiation conditions are described in Section 2.

Nuclide i (half-life)	Number density n_i / (10^{24} cm^{-3})	
	UO_2 fuel	MOX fuel
^{90}Sr (28.8 a)	5.167×10^{-5}	2.519×10^{-5}
^{133}Cs (stable)	7.123×10^{-5}	7.222×10^{-5}
^{134}Cs (2.065 a)	7.538×10^{-6}	7.215×10^{-6}
^{137}Cs (30.07 a)	7.574×10^{-5}	7.735×10^{-5}
^{148}Nd (stable)	2.198×10^{-5}	2.199×10^{-5}
^{149}Sm (stable)	1.590×10^{-7}	3.879×10^{-7}
^{154}Eu (8.60 a)	1.790×10^{-6}	3.246×10^{-6}
^{235}U (7.04×10^{8} a)	2.680×10^{-4}	2.593×10^{-5}
^{236}U (2.342×10^{7} a)	1.625×10^{-4}	6.977×10^{-6}
^{238}U (4.468×10^{9} a)	2.241×10^{-2}	2.159×10^{-2}
^{238}Pu (87.7 a)	9.031×10^{-6}	4.368×10^{-5}
^{239}Pu (2.410×10^{4} a)	2.030×10^{-4}	6.061×10^{-4}
^{240}Pu (6.56×10^{3} a)	6.513×10^{-5}	4.230×10^{-4}
^{241}Pu (14.29 a)	4.491×10^{-5}	2.396×10^{-4}
^{242}Pu (3.75×10^{5} a)	1.643×10^{-5}	1.590×10^{-4}
^{241}Am (432.7 a)	3.422×10^{-6}	2.636×10^{-5}
^{242g}Am (16.02 h)	1.653×10^{-12}	1.710×10^{-11}
^{242m}Am (141 a)	1.281×10^{-7}	1.325×10^{-6}
^{243}Am (7.37×10^{3} a)	3.837×10^{-6}	4.105×10^{-5}
^{242}Cm (0.446 a)	1.136×10^{-7}	8.638×10^{-7}
^{243}Cm (29.1 a)	1.809×10^{-8}	2.004×10^{-7}
^{244}Cm (18.1 a)	1.778×10^{-6}	2.954×10^{-5}

Table A.3: Inventory of nuclides of importance for the characterisation of SNF after irradiation of fresh UO_2 and MOX fuel and a cooling time of 10 a. The composition of the fresh fuel and irradiation conditions are described in Section 2.

Nuclide i (half-life)	Number density n_i / (10^{24} cm^{-3})	
	UO_2 fuel	MOX fuel
^{90}Sr (28.8 a)	4.161×10^{-5}	2.029×10^{-5}
^{133}Cs (stable)	7.123×10^{-5}	7.222×10^{-5}
^{134}Cs (2.065 a)	3.676×10^{-7}	3.518×10^{-7}
^{137}Cs (30.07 a)	6.156×10^{-5}	6.287×10^{-5}
^{148}Nd (stable)	2.198×10^{-5}	2.199×10^{-5}
^{149}Sm (stable)	1.590×10^{-7}	3.879×10^{-7}
^{154}Eu (8.60 a)	1.132×10^{-6}	2.208×10^{-6}
^{235}U (7.04×10^{8} a)	2.681×10^{-4}	2.608×10^{-5}
^{236}U (2.342×10^{7} a)	1.626×10^{-4}	7.383×10^{-6}
^{238}U (4.468×10^{9} a)	2.241×10^{-2}	2.159×10^{-2}
^{238}Pu (87.7 a)	8.521×10^{-6}	4.153×10^{-5}
^{239}Pu (2.410×10^{4} a)	2.030×10^{-4}	6.060×10^{-4}
^{240}Pu (6.56×10^{3} a)	6.559×10^{-5}	4.312×10^{-4}
^{241}Pu (14.29 a)	2.902×10^{-5}	1.549×10^{-4}
^{242}Pu (3.75×10^{5} a)	1.643×10^{-5}	1.590×10^{-4}
^{241}Am (432.7 a)	1.914×10^{-5}	1.101×10^{-4}
^{242g}Am (16.02 h)	1.581×10^{-12}	1.636×10^{-11}
^{242m}Am (141 a)	1.225×10^{-7}	1.268×10^{-6}
^{243}Am (7.37×10^{3} a)	3.833×10^{-6}	4.101×10^{-5}
^{242}Cm (0.446 a)	3.203×10^{-10}	3.313×10^{-9}
^{243}Cm (29.1 a)	1.460×10^{-8}	1.617×10^{-7}
^{244}Cm (18.1 a)	1.260×10^{-6}	2.093×10^{-5}

Table A.4: Inventory of nuclides of importance for the characterisation of SNF after irradiation of fresh UO_2 and MOX fuel and a cooling time of 20 a. The composition of the fresh fuel and irradiation conditions are described in Section 2.

Nuclide i (half-life)	Number density n_i / (10^{24} cm^{-3})	
	UO_2 fuel	MOX fuel
^{90}Sr (28.8 a)	3.270×10^{-5}	1.594×10^{-5}
^{133}Cs (stable)	7.123×10^{-5}	7.222×10^{-5}
^{134}Cs (2.065 a)	1.282×10^{-8}	1.227×10^{-8}
^{137}Cs (30.07 a)	4.889×10^{-5}	4.993×10^{-5}
^{148}Nd (stable)	2.198×10^{-5}	2.199×10^{-5}
^{149}Sm (stable)	1.590×10^{-7}	3.879×10^{-7}
^{154}Eu (8.60 a)	3.872×10^{-7}	7.020×10^{-7}
^{235}U (7.04×10^{8} a)	2.682×10^{-4}	2.626×10^{-5}
^{236}U (2.342×10^{7} a)	1.627×10^{-4}	7.842×10^{-6}
^{238}U (4.468×10^{9} a)	2.241×10^{-2}	2.159×10^{-2}
^{238}Pu (87.7 a)	7.878×10^{-6}	3.842×10^{-5}
^{239}Pu (2.410×10^{4} a)	2.029×10^{-4}	6.059×10^{-4}
^{240}Pu (6.56×10^{3} a)	6.592×10^{-5}	4.374×10^{-4}
^{241}Pu (14.29 a)	1.787×10^{-5}	9.535×10^{-5}
^{242}Pu (3.75×10^{5} a)	1.643×10^{-5}	1.590×10^{-4}
^{241}Am (432.7 a)	2.989×10^{-5}	1.674×10^{-4}
^{242g}Am (16.02 h)	1.505×10^{-12}	1.557×10^{-11}
^{242m}Am (141 a)	1.167×10^{-7}	1.207×10^{-6}
^{243}Am (7.37×10^{3} a)	3.830×10^{-6}	4.098×10^{-5}
^{242}Cm (0.446 a)	3.048×10^{-10}	3.154×10^{-9}
^{243}Cm (29.1 a)	1.150×10^{-8}	1.274×10^{-7}
^{244}Cm (18.1 a)	8.594×10^{-7}	1.428×10^{-5}

Table A.5: Inventory of nuclides of importance for the characterisation of SNF after irradiation of fresh UO_2 and MOX fuel and a cooling time of 30 a. The composition of the fresh fuel and irradiation conditions are described in Section 2.

Nuclide i (half-life)	Number density n_i / (10^{24} cm^{-3})	
	UO_2 fuel	MOX fuel
^{90}Sr (28.8 a)	2.571×10^{-5}	1.253×10^{-5}
^{133}Cs (stable)	7.123×10^{-5}	7.222×10^{-5}
^{134}Cs (2.065 a)	4.468×10^{-10}	4.277×10^{-10}
^{137}Cs (30.07 a)	3.883×10^{-5}	3.965×10^{-5}
^{148}Nd (stable)	2.198×10^{-5}	2.199×10^{-5}
^{149}Sm (stable)	1.590×10^{-7}	3.879×10^{-7}
^{154}Eu (8.60 a)	1.730×10^{-7}	3.136×10^{-7}
^{235}U (7.04×10^{8} a)	2.682×10^{-4}	2.643×10^{-5}
^{236}U (2.342×10^{7} a)	1.627×10^{-4}	8.307×10^{-6}
^{238}U (4.468×10^{9} a)	2.241×10^{-2}	2.159×10^{-2}
^{238}Pu (87.7 a)	7.284×10^{-6}	3.555×10^{-5}
^{239}Pu (2.410×10^{4} a)	2.029×10^{-4}	6.058×10^{-4}
^{240}Pu (6.56×10^{3} a)	6.612×10^{-5}	4.415×10^{-4}
^{241}Pu (14.29 a)	1.100×10^{-5}	5.871×10^{-5}
^{242}Pu (3.75×10^{5} a)	1.643×10^{-5}	1.590×10^{-4}
^{241}Am (432.7 a)	3.622×10^{-5}	2.010×10^{-4}
^{242g}Am (16.02 h)	1.433×10^{-12}	1.483×10^{-11}
^{242m}Am (141 a)	1.111×10^{-7}	1.149×10^{-6}
^{243}Am (7.37×10^{3} a)	3.826×10^{-6}	4.094×10^{-5}
^{242}Cm (0.446 a)	2.902×10^{-10}	3.002×10^{-9}
^{243}Cm (29.1 a)	9.065×10^{-9}	1.004×10^{-7}
^{244}Cm (18.1 a)	5.861×10^{-7}	5.737×10^{-6}

Appendix B. Decay heat rate tables

Table B.1: Nuclides with a substantial contribution to the decay heat of a SNF sample after irradiation of fresh UO_2 and MOX fuels and at cooling time of 1 a. The composition of the fresh fuel and irradiation conditions are described in Section 2. Contributions to the decay heat from decay products with a half-live shorter than 30 d are added to the decay heat of the initial nuclide.

UO_2 fuel		MOX fuel	
Nuclide i	Decay heat rate density p_{ri} / (W/cm^3)	Nuclide i	Decay heat rate density p_{ri} / (W/cm^3)
^{144}Ce/^{144}Pr	0.05521	^{106}Ru/^{106}Rh	0.07391
^{106}Ru/^{106}Rh	0.03876	^{144}Ce/^{144}Pr	0.04618
^{134}Cs	0.02207	^{242}Cm	0.04235
^{90}Sr/^{90}Y	7.132×10^{-3}	^{244}Cm	0.03388
^{137}Cs/^{137m}Ba	6.931×10^{-3}	^{134}Cs	0.02113
^{242}Cm	5.569×10^{-3}	^{238}Pu	9.797×10^{-3}
^{95}Nb	4.203×10^{-3}	^{137}Cs/^{137m}Ba	7.078×10^{-3}
^{95}Zr	2.045×10^{-3}	^{95}Nb	3.561×10^{-3}
^{244}Cm	2.039×10^{-3}	^{90}Y/^{90}Sr	3.477×10^{-3}
^{238}Pu	2.026×10^{-3}	^{154}Eu	2.013×10^{-3}
total	0.1512	total	0.2526

Table B.2: Nuclides with a substantial contribution to the decay heat of a SNF sample after irradiation of fresh UO_2 and MOX fuels and at cooling time of 10 a. The composition of the fresh fuel and irradiation conditions are described in Section 2. Contributions to the decay heat from decay products with a half-live shorter than 30 d are added to the decay heat of the initial nuclide.

UO_2 fuel		MOX fuel	
Nuclide i	Decay heat rate density p_{ri} / (W/cm^3)	Nuclide i	Decay heat rate density p_{ri} / (W/cm^3)
^{90}Sr/^{90}Y	5.742×10^{-3}	^{244}Cm	0.02401
^{137}Cs/^{137m}Ba	5.633×10^{-3}	^{238}Pu	9.315×10^{-3}
^{238}Pu	1.911×10^{-3}	^{137}Cs/^{137m}Ba	5.753×10^{-3}
^{244}Cm	1.440×10^{-3}	^{241}Am	5.041×10^{-3}
^{134}Cs	1.076×10^{-3}	^{90}Sr/^{90}Y	2.799×10^{-3}
^{241}Am	8.761×10^{-4}	^{240}Pu	1.215×10^{-3}
^{154}Eu	5.375×10^{-4}	^{134}Cs	1.030×10^{-3}
^{240}Pu	1.848×10^{-4}	^{154}Eu	9.745×10^{-4}
^{239}Pu	1.554×10^{-4}	^{239}Pu	4.638×10^{-4}
^{85}Kr	1.116×10^{-4}	^{241}Pu	2.043×10^{-4}
total	0.01814	total	0.05178

Table B.3: Nuclides with a substantial contribution to the decay heat of a SNF sample after irradiation of fresh UO_2 and MOX fuels and at cooling time of 20 a. The composition of the fresh fuel and irradiation conditions are described in Section 2. Contributions to the decay heat from decay products with a half-live shorter than 30 d are added to the decay heat of the initial nuclide.

UO_2 fuel		MOX fuel	
Nuclide i	Decay heat rate density p_{ri} / (W/cm^3)	Nuclide i	Decay heat rate density p_{ri} / (W/cm^3)
^{90}Sr/^{90}Y	4.513×10^{-3}	^{244}Cm	0.01637
^{137}Cs/^{137m}Ba	4.474×10^{-3}	^{238}Pu	8.618×10^{-3}
^{238}Pu	1.767×10^{-3}	^{241}Am	7.662×10^{-3}
^{241}Am	1.368×10^{-3}	^{137}Cs/^{137m}Ba	4.569×10^{-3}
^{244}Cm	9.854×10^{-4}	^{90}Sr/^{90}Y	2.200×10^{-3}
^{154}Eu	2.401×10^{-4}	^{240}Pu	1.232×10^{-3}
^{240}Pu	1.857×10^{-4}	^{239}Pu	4.637×10^{-4}
^{239}Pu	1.553×10^{-4}	^{154}Eu	4.353×10^{-4}
^{85}Kr	6.081×10^{-5}	^{242}Cm	1.546×10^{-4}
^{134}Cs	3.753×10^{-5}	^{241}Pu	1.258×10^{-4}
total	0.01399	total	0.04229

Table B.4: Nuclides with a substantial contribution to the decay heat of a SNF sample after irradiation of fresh UO_2 and MOX fuels and at cooling time of 30 a. The composition of the fresh fuel and irradiation conditions are described in Section 2. Contributions to the decay heat from decay products with a half-live shorter than 30 d are added to the decay heat of the initial nuclide.

UO_2 fuel		MOX fuel	
Nuclide i	Decay heat rate density p_{ri} / (W/cm^3)	Nuclide i	Decay heat rate density p_{ri} / (W/cm^3)
^{90}Sr/^{90}Y	3.548×10^{-3}	^{244}Cm	0.01117
^{137}Cs/^{137m}Ba	3.553×10^{-3}	^{241}Am	9.204×10^{-3}
^{241}Am	1.658×10^{-3}	^{238}Pu	7.974×10^{-3}
^{238}Pu	1.634×10^{-3}	^{137}Cs/^{137m}Ba	3.629×10^{-3}
^{244}Cm	6.720×10^{-4}	^{90}Sr/^{90}Y	1.730×10^{-3}
^{240}Pu	1.863×10^{-4}	^{240}Pu	1.244×10^{-3}
^{239}Pu	1.553×10^{-4}	^{239}Pu	4.637×10^{-4}
^{154}Eu	1.072×10^{-4}	^{154}Eu	1.944×10^{-4}
^{85}Kr	3.192×10^{-5}	^{242}Cm	1.472×10^{-4}
^{241}Pu	1.451×10^{-5}	^{243}Am	1.062×10^{-4}
total	0.01171	total	0.03618

GETTING IN TOUCH WITH THE EU

In person

All over the European Union there are hundreds of Europe Direct information centres. You can find the address of the centre nearest you at: http://europea.eu/contact

On the phone or by email

Europe Direct is a service that answers your questions about the European Union. You can contact this service:

- by freephone: 00 800 6 7 8 9 10 11 (certain operators may charge for these calls),

- at the following standard number: +32 22999696, or

- by electronic mail via: http://europa.eu/contact

FINDING INFORMATION ABOUT THE EU

Online

Information about the European Union in all the official languages of the EU is available on the Europa website at: http://europa.eu

EU publications
You can download or order free and priced EU publications from EU Bookshop at: http://bookshop.europa.eu. Multiple copies of free publications may be obtained by contacting Europe Direct or your local information centre (see http://europa.eu/contact).

KJ-NA-29301-EN-N

JRC Mission

As the science and knowledge service of the European Commission, the Joint Research Centre's mission is to support EU policies with independent evidence throughout the whole policy cycle.

EU Science Hub
ec.europa.eu/jrc

@EU_ScienceHub

EU Science Hub - Joint Research Centre

Joint Research Centre

EU Science Hub

Publications Office

doi:10.2760/418524

ISBN 978-92-79-90347-2